AIAA/CEAS 13. Aeroacoustics Conference, Roma, (ITA), May 21–23, 2007

Pressure, Density and Temperature Fluctuations in Compressible Turbulent Flow — I

G.A. Gerolymos,* D. Sénéchal,† and I. Vallet‡
Université Pierre-et-Marie-Curie, 75005 Paris, France

The purpose of the present paper is to study pressure fluctuations in subsonic flows, analyzing compressible channel flow DNS computations. The transport equation for $\overline{p'^2}$ is studied. The coupling of pressure fluctuations with density and temperature fluctuations (which are related through the equation of state) is discussed, for various Mach-numbers. Budgets of the various terms appearing in the transport equation for $\overline{p'^2}$ are presented, and closures of the various terms are compared with DNS data. The limiting form of the transport equation for $\overline{p'^2}$ for $M \longrightarrow 0$ is used to suggest a possible explanation of the well-known Reynolds-number dependence of wall-pressure-variance. Then scaling of wavenumber-frequency wall-pressure spectra on local flow variables is discussed. The possibility of using these results in a broadband noise prediction methodology is assessed.

I. Introduction

Pressure-fluctuations (p'), in wall-bounded flows, have been studied extensively using incompressible DNS computations.[1–4] Within the assumption of incompressibility, pressure fluctuations are related to integrals of velocity-gradients and velocity-gradients-fluctuations, through the well known Poisson equation for pressure.[5] Kim[6] used a Green's function approach,[7] as a part of DNS computations postprocessing, to analystically solve the Poisson equations corresponding to the slow (turbulence/turbulence) and rapid (turbulence/mean-flow-gradient) source-terms. This method has been used by Chang et al.[1] for the detailed study of pressure fluctuations in incompressible turbulent channel flow, and by Foysi et al.[8] for compressible channel flows. The present authors[9] have extended the Green's function methodology to investigate the wall-blockage effect on p',[10] for each of the 10 source-terms of compressible flow the Poisson equation for p'.

The knowledge of the pressure-fluctuation field (and of its wavenumber-frequency spectra) is essential in aeroacoustic predictions of broadband noise, and it is highly desirable to develop a model capable of extracting this information from RANS computations (with advanced turbulence-anisotropy-resolving models).[11] Short of various approaches based on synthetic turbulence generation coupled with the solution of the Poisson equation for p' (limited to incompressible flow),[12] there is indeed very little work on the development of general field models for $\overline{p'^2}$ (or $[p'_{\rm rms}]^2 := \overline{p'^2}$). In a rather obscure paper, Chen[13] developed a transport equation for $p'_{\rm rms}$, with plausible results in plane channel flow (although, because of the wall-boundary-condition used for $p'_{\rm rms}$, the model is incapable of mimicking the Re_{τ_w}-dependence of $[p'_{\rm rms}]_w$). The approach followed by Chen contains many arbitrary *ad hoc* assumptions, mainly because, in strictly incompressible flow there is no exact transport equation for the static pressure. However, even for low-Mach-number aeroacoustics, an exact transport equation for $p'_{\rm rms}$ can be developed, by considering that the flow is (weakly) compressible (which is indeed the case). Notice that the homogeneous shear flow version of this equation was used by Hamba,[14] to model the pressure-dilatation correlation in high-speed flows (in the absence of solid walls).

In the present paper the $\overline{p'^2}$-transport equation is examined, based on data from compressible channel flow DNS computations.[15] Since $\overline{p'^2}$ is coupled with $\overline{\rho'^2}$ and $\widetilde{T''^2}$, through the thermodynamic equation-of-state $p = p(\rho, T)$, the transport equations for $\overline{\rho'^2}$ and $\widetilde{T''^2}$ are studied as well. Budgets of these equations are given and modelling approaches are suggested for the various terms. The relation of pressure, density and temperature fluctuations is studied. Then the possibility of developping a scaling of wall-pressure spectra based on local data is discussed.

*Professor, Institut d'Alembert, Case 161, 4 place Jussieu, e-mail: geg@ccr.jussieu.fr
†Research Assistant, Institut d'Alembert, Case 161, 4 place Jussieu, e-mail: dsenecha@ccr.jussieu.fr
‡Assistant Professor, Institut d'Alembert, Case 161, 4 place Jussieu, e-mail: vallet@ccr.jussieu.fr

II. Pressure-Fluctuations Transport

A. Basic Flow-Equations

Starting from the conservation equations

$$\frac{\partial \rho}{\partial t} + \frac{\partial}{\partial x_\ell}[\rho u_\ell] = 0 \tag{1}$$

$$\frac{\partial \rho u_i}{\partial t} + \frac{\partial}{\partial x_\ell}[\rho u_i u_\ell] = -\frac{\partial p}{\partial x_i} + \frac{\partial \tau_{i\ell}}{\partial x_\ell} + \rho f_{\mathrm{v}_i} \tag{2}$$

$$\frac{\partial}{\partial t}[\rho h_t - p] + \frac{\partial}{\partial x_\ell}[\rho h_t u_\ell] = \frac{\partial}{\partial x_\ell}[u_m \tau_{m\ell} - q_\ell] + \rho f_{\mathrm{v}_m} u_m \tag{3}$$

the static temperature equation may be obtained by substracting the conservation of momentum premultiplied by u_i (Eq. 2) from the total energy equation (Eq. 3)

$$\rho c_p \frac{DT}{Dt} = \beta_p T \frac{Dp}{Dt} + \tau_{m\ell} S_{m\ell} - \frac{\partial q_\ell}{\partial x_\ell} \tag{4}$$

where use was made of the thermodynamic identity

$$dh = c_p dT + \frac{1 - \beta_p T}{\rho} dp \qquad ; \qquad c_p = \left[\frac{\partial h}{\partial T}\right]_p \qquad ; \qquad \beta_p = -\frac{1}{\rho}\left[\frac{\partial \rho}{\partial T}\right]_p \tag{5}$$

The above equations (Eqs. 1–5) are valid for general thermodynamic relations $p = p(\rho, T)$ and $c_p = c_p(\rho, T)$. Using the thermodynamic identity $D_t p \equiv [\partial_\rho p]_T D_t \rho + [\partial_T p]_\rho D_t T$, continuity (Eq. 1) and static-temperature-transport (Eq. 4) can be combined to give the static-pressure-transport equation

$$\frac{Dp}{Dt} = \frac{1}{1 - \dfrac{\beta_p T}{\rho c_p}\left[\dfrac{\partial p}{\partial T}\right]_\rho} \left(-\frac{\rho}{p}\left[\frac{\partial p}{\partial \rho}\right]_T p S_{\ell\ell} + \frac{p}{T \rho c_p}\left[\frac{\partial p}{\partial T}\right]_\rho (\tau_{m\ell} S_{m\ell} - \frac{\partial q_\ell}{\partial x_\ell}) \right) \tag{6}$$

where for a general equation-of-state using a compressibility-factor $Z(\rho, T)$

$$p = \rho R_g T Z \Longrightarrow \begin{cases} \left[\dfrac{\partial p}{\partial \rho}\right]_T = \dfrac{p}{\rho}\left(1 + \dfrac{\rho}{Z}\left[\dfrac{\partial Z}{\partial \rho}\right]_T\right) \\ \left[\dfrac{\partial p}{\partial \rho}\right]_T = \dfrac{p}{\rho}\left(1 + \dfrac{\rho}{Z}\left[\dfrac{\partial Z}{\partial T}\right]_\rho\right) \end{cases} \tag{7}$$

Notice that the volume forces f_{v_i} present in the momentum equation (Eq. 2), appear neither in the static temperature (Eq. 4) nor in the static pressure (Eq. 6) equations.

B. Perfect-Gas Equation-of-State

To simplify the analysis perfect gas thermodynamics with constant c_p will be assumed

$$p = \rho R_g T \qquad ; \qquad Z = 1 \qquad ; \qquad c_p - c_v = R_g \qquad ; \qquad \beta_p = \frac{1}{T} \tag{8}$$

Then the static-pressure-transport equation becomes

$$Z = 1 \Longrightarrow \frac{Dp}{Dt} = -\gamma p S_{\ell\ell} + (\gamma - 1)\tau_{m\ell} S_{m\ell} - (\gamma - 1)\frac{\partial q_\ell}{\partial x_\ell} \tag{9}$$

with $\gamma := c_p / c_v$ the ratio of specific heats. This form of the static-pressure-transport (Eq. 9) has been used by several authors, in lieu of the energy-conservation equation, both in theoretical studies[14] of compressible turbulence, and in DNS computations[16] of shockless compressible flows. As shown in the previous discussion this form of the static-pressure-transport (Eq. 9) is only valid when $Z = 1 \; \forall (\rho, T)$.

In the following, we will further assume $\gamma = \mathrm{const}$, together with standard linear laws for the constitutive relation for the stress-tensor and the heat-flux vector

$$\tau_{ij} = \mu(T)\left[\frac{\partial u_i}{\partial x_j} + \frac{\partial u_j}{\partial x_i} - \tfrac{2}{3}\frac{\partial u_\ell}{\partial x_\ell}\delta_{ij}\right] + \mu_{\mathrm{b}}(T)\frac{\partial u_\ell}{\partial x_\ell}\delta_{ij} \equiv 2\mu(T)\left(S_{ij} - \tfrac{1}{3}S_{\ell\ell}\delta_{ij}\right) + \mu_{\mathrm{b}}(T) S_{\ell\ell}\delta_{ij} \quad ; \quad q_i = -\lambda(T)\frac{\partial T}{\partial x_i} \tag{10}$$

C. The Poisson Equation

Modelling the terms containing the pressure-fluctuation p', *eg* redistribution ϕ_{ij}, pressure diffusion $d_{ij}^{(p)}$, and pressure-dilatation ϕ_p, requires the analysis of the dynamics of p'. This, following Chou,[5] is traditionally based on the incompressible-flow Poisson equation for p', although, several authors,[8,17–20] have contributed towards extending this approach to the compressible flow Poisson equation for p'. There are several equivalent forms, one of which is[9]

$$\begin{aligned}
\nabla^2 p' = {} & \underbrace{\frac{\partial^2 \tau_{ij'}}{\partial x_i \partial x_j}}_{Q'_{(\tau)}} + \underbrace{\frac{\partial}{\partial x_i}(\rho f_{\mathrm{V}_i} - \overline{\rho f_{\mathrm{V}_i}})}_{Q'_{(\mathrm{BF})}} \\
& + \underbrace{\left[-\bar{\rho}\left(\frac{\partial u_i''}{\partial x_j}\frac{\partial u_j''}{\partial x_i} - \overline{\frac{\partial u_i''}{\partial x_j}\frac{\partial u_j''}{\partial x_i}}\right)\right]}_{Q'_{(\mathrm{s})}} + \underbrace{\left[-\left(\rho'\frac{\partial u_i''}{\partial x_j}\frac{\partial u_j''}{\partial x_i} - \overline{\rho'\frac{\partial u_i''}{\partial x_j}\frac{\partial u_j''}{\partial x_i}}\right)\right]}_{Q'_{(\rho'\mathrm{s})}} \\
& + \underbrace{\left[-2\bar{\rho}\left(\frac{\partial u_i''}{\partial x_j} - \frac{\partial \overline{u_i''}}{\partial x_j}\right)\frac{\partial \tilde{u}_j}{\partial x_i}\right]}_{Q'_{(\mathrm{r})}} + \underbrace{\left[-2\left(\rho'\frac{\partial u_i''}{\partial x_j} - \overline{\rho'\frac{\partial u_i''}{\partial x_j}}\right)\frac{\partial \tilde{u}_j}{\partial x_i}\right]}_{Q'_{(\rho'\mathrm{r})}} + \underbrace{\left[-\rho'\frac{\partial \tilde{u}_i}{\partial x_j}\frac{\partial \tilde{u}_j}{\partial x_i}\right]}_{Q'_{(\rho')}} \\
& + \underbrace{\left[-\left(\rho'\overline{\frac{D\Theta}{Dt}} + \rho\left[\frac{D\Theta}{Dt}\right]' - \overline{\rho'\frac{D\Theta'}{Dt}}\right)\right]}_{Q'_{(\Theta)}} + \underbrace{\left[-\left(\left[\frac{Du_i}{Dt}\right]'\frac{\partial \bar{\rho}}{\partial x_i}\right)\right]}_{Q'_{(\dot{V}\nabla\bar{\rho})}} + \underbrace{\left[-\left(\frac{Du_i}{Dt}\frac{\partial \rho'}{\partial x_i} - \overline{\left[\frac{Du_i}{Dt}\right]'\frac{\partial \rho'}{\partial x_i}}\right)\right]}_{Q'_{(\dot{V}\nabla\rho')}}
\end{aligned} \tag{11}$$

This equation, which for the plane channel flow case may be easily solved using the appropriate Green's function,[6,9] has been used by many authors to investigate the relative importance of various mechanisms (*eg* rapid and slow,[1] density fluctuation and mean gradient influence,[8] wall-echo effects on the various source-mechanisms,[9] $\cdots$).

D. Pressure-Variance Transport

Alternatively, the transport equation for $\overline{p'^2}$ may be used. After some straightforward algebra, the transport equation for the pressure-variance is obtained

$$\begin{aligned}
\underbrace{\frac{\partial \overline{p'^2}}{\partial t} + \bar{u}_\ell\frac{\partial \overline{p'^2}}{\partial x_\ell}}_{\text{convection } C_{p'}} = {} & \underbrace{-2\overline{p'u'_\ell}\frac{\partial \bar{p}}{\partial x_\ell}}_{\text{production } P_{(p';\nabla\bar{p})}} \quad \underbrace{+4(\gamma-1)\bar{\mu}\phi_{m\ell}\frac{\partial \bar{u}_m}{\partial x_\ell}}_{\text{production } P_{(p';\phi_{ij})}} \quad \underbrace{-2\gamma\overline{p'^2}\frac{\partial \bar{u}_\ell}{\partial x_\ell}}_{\text{production } P_{(p';\bar{\Theta})}} \\
& \underbrace{-(2\gamma-1)\overline{p'^2\frac{\partial u'_\ell}{\partial x_\ell}} - 3\left[\gamma\bar{p} - 2(\gamma-1)\bar{\mu}_\mathrm{b}\frac{\partial \bar{u}_\ell}{\partial x_\ell}\right]\phi_p}_{\text{dilatation fluctuations } K_{(p';\Theta')}} \quad \underbrace{-2(\gamma-1)\bar{\lambda}\overline{\frac{\partial p'}{\partial x_\ell}\frac{\partial T'}{\partial x_\ell}}}_{\text{destruction } \varepsilon_{(p')}} \\
& \underbrace{+2(\gamma-1)\left[\bar{\mu}p'\overline{\frac{\partial u'_m}{\partial x_\ell}\frac{\partial u'_m}{\partial x_\ell}} + \bar{\mu}p'\overline{\frac{\partial u'_\ell}{\partial x_m}\frac{\partial u'_m}{\partial x_\ell}} - (\tfrac{2}{3}\bar{\mu} - \bar{\mu}_\mathrm{b})p'\overline{\frac{\partial u'_\ell}{\partial x_\ell}\frac{\partial u'_m}{\partial x_m}}\right]}_{\text{triple correlations } E_{(p')}} \\
& \underbrace{+\frac{\partial}{\partial x_\ell}\left[-\overline{p'^2u'_\ell} + 2(\gamma-1)\bar{\lambda}p'\overline{\frac{\partial T'}{\partial x_\ell}}\right]}_{\text{diffusion } d_{(p')} = d^{(u)}_{(p')} + d^{(\lambda)}_{(p')}} \quad +(\mu' \text{ and } \lambda' \text{ terms})
\end{aligned} \tag{12}$$

where ϕ_{ij} is the redistribution tensor and ϕ_p is the pressure-dilatation correlation

$$\phi_{ij} = \overline{p'\left(\frac{\partial u'_i}{\partial x_j} + \frac{\partial u'_j}{\partial x_i} - \tfrac{2}{3}\frac{\partial u'_\ell}{\partial x_\ell}\delta_{ij}\right)} \quad ; \quad \phi_p = \tfrac{2}{3}\overline{p'\frac{\partial u'_\ell}{\partial x_\ell}} \tag{13}$$

A similar equation has been studied by Hamba,[14] but omitting the correlations associated with τ'_{ij} (terms $P_{(p';\phi_{ij})}$ and $E_{(p')}$; Eq. 12). This approximation is acceptable in the case of homogeneous turbulence, far from solid walls studied by Hamba,[14] but not in the present case, where we are interested in the near-wall strongly inhomogeneous region.

E. Density-Variance Transport

The density-variance ($\overline{\rho'^2}$) transport equation is obtained after some straightforward algebra[14,18] from the continuity equation (Eq. 1)

$$\underbrace{\frac{\partial\overline{\rho'^2}}{\partial t}+\tilde{u}_\ell\frac{\partial\overline{\rho'^2}}{\partial x_\ell}}_{\text{convection } C_{(\rho')}} = \underbrace{\frac{\partial\left(-\overline{\rho'^2u''_\ell}\right)}{\partial x_\ell}}_{\text{diffusion } d_{(\rho')}} \underbrace{-2\overline{\rho' u'_\ell}\frac{\partial\bar{\rho}}{\partial x_\ell}-2\overline{\rho'^2}\frac{\partial\tilde{u}_\ell}{\partial x_\ell}}_{\text{production } P_{(\rho')}:=P_{(\rho';\nabla\bar{\rho})}+P_{(\rho';\breve{\Theta})}} - \underbrace{\left[-\overline{\rho'^2\frac{\partial u''_\ell}{\partial x_\ell}}+2\overline{\rho\rho'\frac{\partial u''_\ell}{\partial x_\ell}}\right]}_{\text{destruction } \varepsilon_{(\rho')}:=\varepsilon_{(\rho';1)}+\varepsilon_{(\rho';2)}} \tag{14}$$

where the identity $\overline{\mathrm{a'b''}}=\overline{\mathrm{a'b''}}=\overline{\mathrm{a'b''}}$, valid[21,22] for any 2 flow-quantities a and b, was used. The present form is the one given by Taulbee and VanOsdol.[18] Other alternative expressions are possible,[23] and will be discussed along with the analysis of budgets and modelling of the density-variance-equation (§IV.B).

There are (Eq. 14) 2 mechanisms of interaction with meanflow-gradients which can produce density-fluctuations. The first mechanism is the production of $\overline{\rho'^2}$ by the action of the fluctuating-massflux with grad$\bar{\rho}$ ($P_{(\rho';\nabla\bar{\rho})}$; Eq. 14). It is expected that in most flow situations $P_{(\rho';\nabla\bar{\rho})}\geq 0$. The second mechanism ($P_{(\rho';\breve{\Theta})}$; Eq. 14) is related to meanflow-dilatation $\breve{\Theta}=\partial_{x_\ell}\tilde{u}_\ell$. Since $\overline{\rho'^2}\geq 0$ this mechanisms produces ρ', *eg* in decelerating flow ($\breve{\Theta}<0$), and destroys ρ' in accelerating flow ($\breve{\Theta}>0$).

F. Temperature-Variance Transport

The temperature-variance ($\widetilde{T''^2}$) transport equation is obtained after some straightforward algebra

$$\begin{aligned}\underbrace{\frac{\partial\bar{\rho}\widetilde{T''T''}}{\partial t}+\frac{\partial\tilde{u}_\ell\bar{\rho}\widetilde{T''T''}}{\partial x_\ell}}_{\text{convection } C_{(T'')}} = & \underbrace{-2\bar{\rho}\widetilde{u''_\ell T''}\frac{\partial\tilde{T}}{\partial x_\ell}}_{\text{production } P_{(T'';\nabla\bar{T})}} \underbrace{-2\frac{(\gamma-1)}{R_g}\overline{T'p'}\frac{\partial\bar{u}_\ell}{\partial x_\ell}}_{\text{production } P_{(T'';\bar{\Theta})}} \underbrace{+4\frac{(\gamma-1)}{R_g}\bar{\mu}\overline{T'\frac{\partial u'_m}{\partial x_\ell}}\left(\frac{\partial\bar{u}_m}{\partial x_\ell}+\frac{\partial\bar{u}_\ell}{\partial x_m}\right)}_{\text{production } P_{(T'';\bar{\tau}_{ij})}} \\ & \underbrace{+\frac{\partial}{\partial x_\ell}\left[-\bar{\rho}\widetilde{u''_\ell T''T''}+\frac{(\gamma-1)}{R_g}\bar{\lambda}\overline{\frac{\partial T'T'}{\partial x_\ell}}\right]}_{\text{diffusion } d_{(T'')}=d^{(u)}_{(T'')}+d^{(\lambda)}_{(T'')}} \underbrace{-2\frac{(\gamma-1)}{R_g}\bar{\lambda}\overline{\frac{\partial T'}{\partial x_\ell}\frac{\partial T'}{\partial x_\ell}}}_{\text{destruction } \varepsilon_{(T'')}} \\ & \underbrace{-2\frac{(\gamma-1)}{R_g}\overline{T''p'\frac{\partial u'_\ell}{\partial x_\ell}}-2\frac{(\gamma-1)}{R_g}\left[\bar{p}+2\left(\tfrac{2}{3}\bar{\mu}-\bar{\mu}_\mathrm{b}\right)\frac{\partial\bar{u}_m}{\partial x_m}\right]\overline{T'\frac{\partial u'_\ell}{\partial x_\ell}}}_{\text{dilatation fluctuations } K_{(T'';\Theta')}} \\ & \underbrace{+2\frac{(\gamma-1)}{R_g}\overline{T''}\left[\bar{\mu}\frac{\partial\bar{u}_m}{\partial x_\ell}\frac{\partial\bar{u}_m}{\partial x_\ell}+\bar{\mu}\frac{\partial\bar{u}_\ell}{\partial x_m}\frac{\partial\bar{u}_m}{\partial x_\ell}-(\tfrac{2}{3}\bar{\mu}-\bar{\mu}_\mathrm{b})\frac{\partial\bar{u}_\ell}{\partial x_\ell}\frac{\partial\bar{u}_m}{\partial x_m}-\bar{p}\frac{\partial\bar{u}_\ell}{\partial x_\ell}+\frac{\partial}{\partial x_\ell}\left(\bar{\lambda}\frac{\partial\bar{T}}{\partial x_\ell}\right)\right]}_{\text{compressibility effects } K_{(T'')}} \\ & \underbrace{+2\frac{(\gamma-1)}{R_g}\left[\bar{\mu}\overline{T''\frac{\partial u'_m}{\partial x_\ell}\frac{\partial u'_m}{\partial x_\ell}}+\bar{\mu}\overline{T''\frac{\partial u'_\ell}{\partial x_m}\frac{\partial u'_m}{\partial x_\ell}}-(\tfrac{2}{3}\bar{\mu}-\bar{\mu}_\mathrm{b})\overline{T''\frac{\partial u'_\ell}{\partial x_\ell}\frac{\partial u'_m}{\partial x_m}}\right]}_{\text{triple correlations } E_{(T'')}} \\ & +(\mu' \text{ and } \lambda' \text{ terms})\end{aligned} \tag{15}$$

A similar equation has been studied by Tamano and Morinishi.[24]

III. DNS Computations

Turbulent channel flow DNS results exist either for incompressible[25,26] or for supersonic[8,27] flow, but to the authors knowledge the actual coupling fluctuating pressure, density, and temperature fields in subsonic channel (wall-bounded) flow has not been studied in detail (Foosi et al.[8] computed [$Re_{\tau_w} = 180$, $M_{\mathrm{B}} = 0.3$] flow, but focussed their invvestigation on the compressibility effects on the Reynolds-stress redistribution tensor ϕ_{ij}). To examine the various terms appearing in the previous transport equation for $\overline{p'^2}$, compressible channel flow[27] DNS computations were performed for $Re_{\tau_w} = 180, 230$, and for $M_{\mathrm{B}_w} = 0.3, 1.5$.

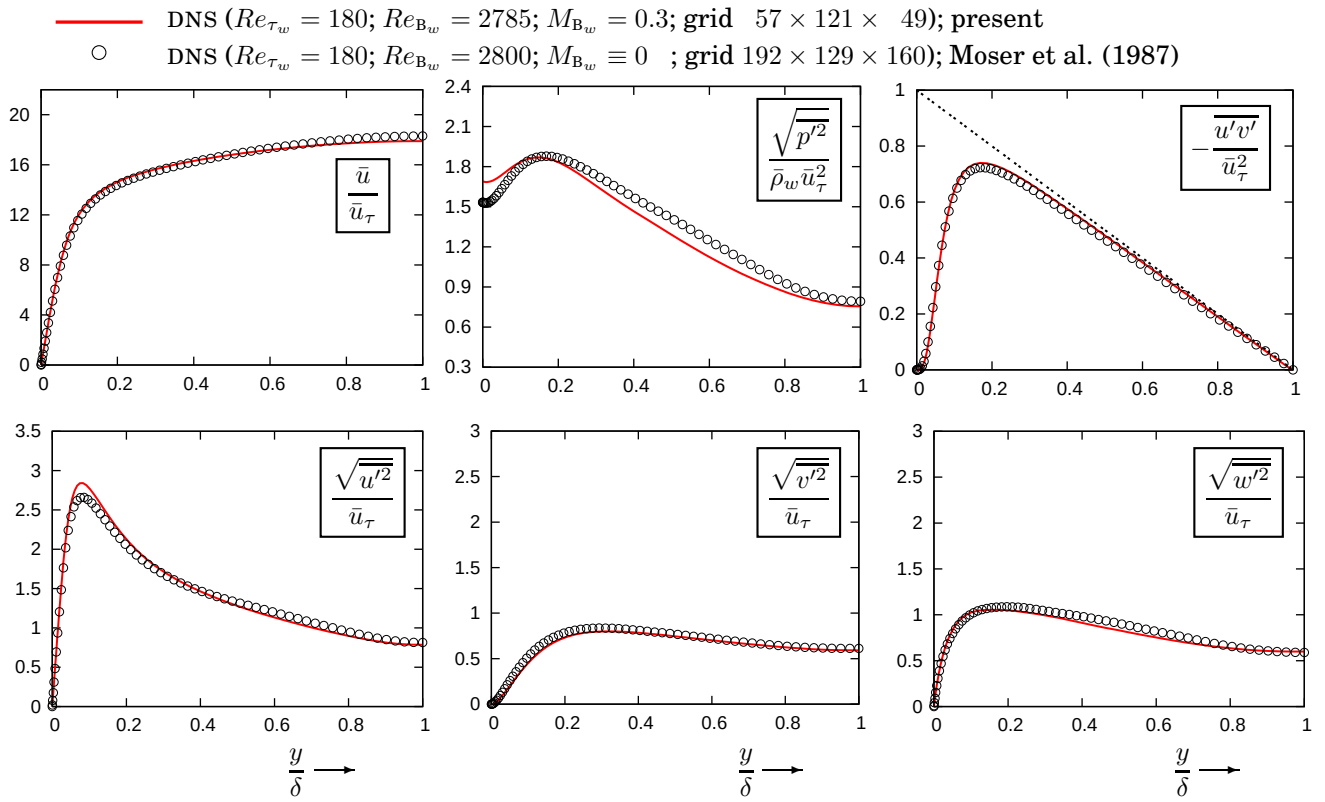

Figure 1. Comparison of present DNS[15] computed statistics ($Re_{\tau_w} = 180$; $M_{\mathrm{B}_w} = 0.3$ with incompressible DNS results of Kim et al.[25,26] ($Re_{\tau_w} = 180$; $M_{\mathrm{B}_w} \equiv 0$).

The DNS solver uses high-order ($O(\Delta x_{\mathrm{H}}^9)$ low-diffusion upwind schemes,[15,22] and implicit $O(\Delta t^2)$ dual-time-stepping time-integration with explicit subiterations,[15,22,28] to solve the conservation equations (Eqs. 1–3). The previously mentionned thermodynamic and constitutive relations were used (Eqs. 8, 10) with a Sutherland law for μ and a modified Sutherland law for λ, with standard values for air.[29] The bulk-viscosity coefficient was set to 0 ($\mu_{\mathrm{b}} = 0$), in accordance with most compressible flow channel DNS computations.[8,27,30] A rather coarse baseline grid was used for the present assessment.[22] The statistics obtained with these DNS computations were validated by comparison with both incompressible[2,4,25,26,31] (Fig. 1), and with compressible[8,27] (Fig. 2) DNS data.

IV. Analysis of the DNS Results

A. Variances and Correlation Coefficients

Examination of the variances of pressure, temperature and density, normalized by the local mean values of the corresponding variables (Fig. 3) indicates that the relative level of fluctuation is comparable for all of the 3 thermodynamic variables. Examination of the correlation coefficients $C_{p\rho}$, $C_{\rho T}$, C_{pT} (where for any flow variables a and b the correlation coefficient is defined as[33] $C_{ab} \doteq \overline{a'b'}/a_{\mathrm{rms}}b_{\mathrm{rms}}$) indicates (Fig. 3) that, near the wall pressure and temperature (C_{pT}) are almost uncorrelated, the correlation increasing towards midchannel (Fig. 3). Density and temperature are uncorrelated at the wall, but the correlation rapidly increases (in absolute value) towards $C_{\rho T} = -1$, and then falls towards midchannel. Pressure and density are

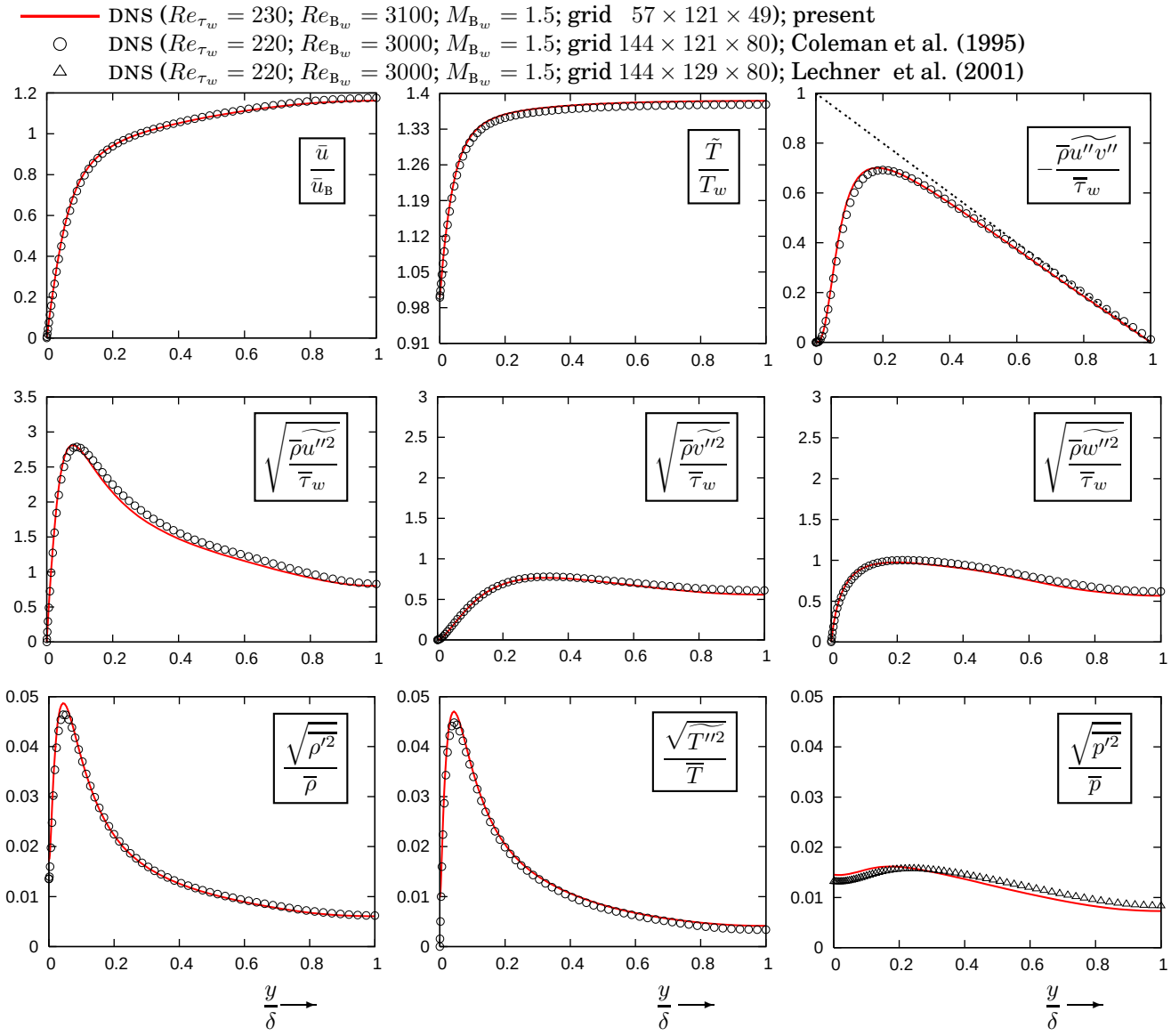

Figure 2. Comparison of computed turbulence statistics from present DNS computations using the HLLCB–UW9 scheme, with DNS results of Coleman et al.[27,32] and of Lechner et al.,[30] for the turbulent compressible channel flow of Coleman et al.[27,30,32] ($Re_{B_w} = 3100$, $M_{B_w} = 1.5$, isothermal walls).

fully correlated at the wall, with a decrease and subsequent increase towards midchannel (Fig. 3). Both the high-Mach-number results ($\bar{M}_{B_w} = 1.5$; $\bar{M}_{CL} = 1.5$) and the low-Mach-number results ($\bar{M}_{B_w} = 0.3$; $\bar{M}_{CL} = 0.34$) bring forward the strong coupling between pressure and density fluctuations (Fig. 3) which is induced by the isothermal wall-boundary-condition

$$T'_w \equiv 0 \iff \rho'_w = \frac{\gamma p'_w}{\bar{a}_w^2} \tag{16}$$

This isothermal-wall boundary-condition obviously induces a correlation coefficient $[C_{p\rho}]_w = 1$ (Fig. 3). Notice that the ratios $\rho'_{rms}/\bar{\rho}$ and $T'_{rms}/\bar{T}$ exhibit a peak at $y^+ \in [8, 9]$, contrary to the distribution of $p'_{rms}/\bar{p}$ whose maximum is located at $y^+ \in [25, 28]$, and which is quite flat in the entire range $y^+ \in [0, 30]$ The only noticeable Mach-number-influence is that the correlation between density and temperature drops to $C_{\rho T} \cong 0$ in the midchannel region for $\bar{M}_{CL} = 0.34$, whereas it has a value of $C_{\rho T} \cong 0.25$ for $\bar{M}_{CL} = 1.5$ (Fig. 3), with an associated small difference in the level of the other 2 corelations.

To better understand the implications of the above results, use is made of the following relations, which

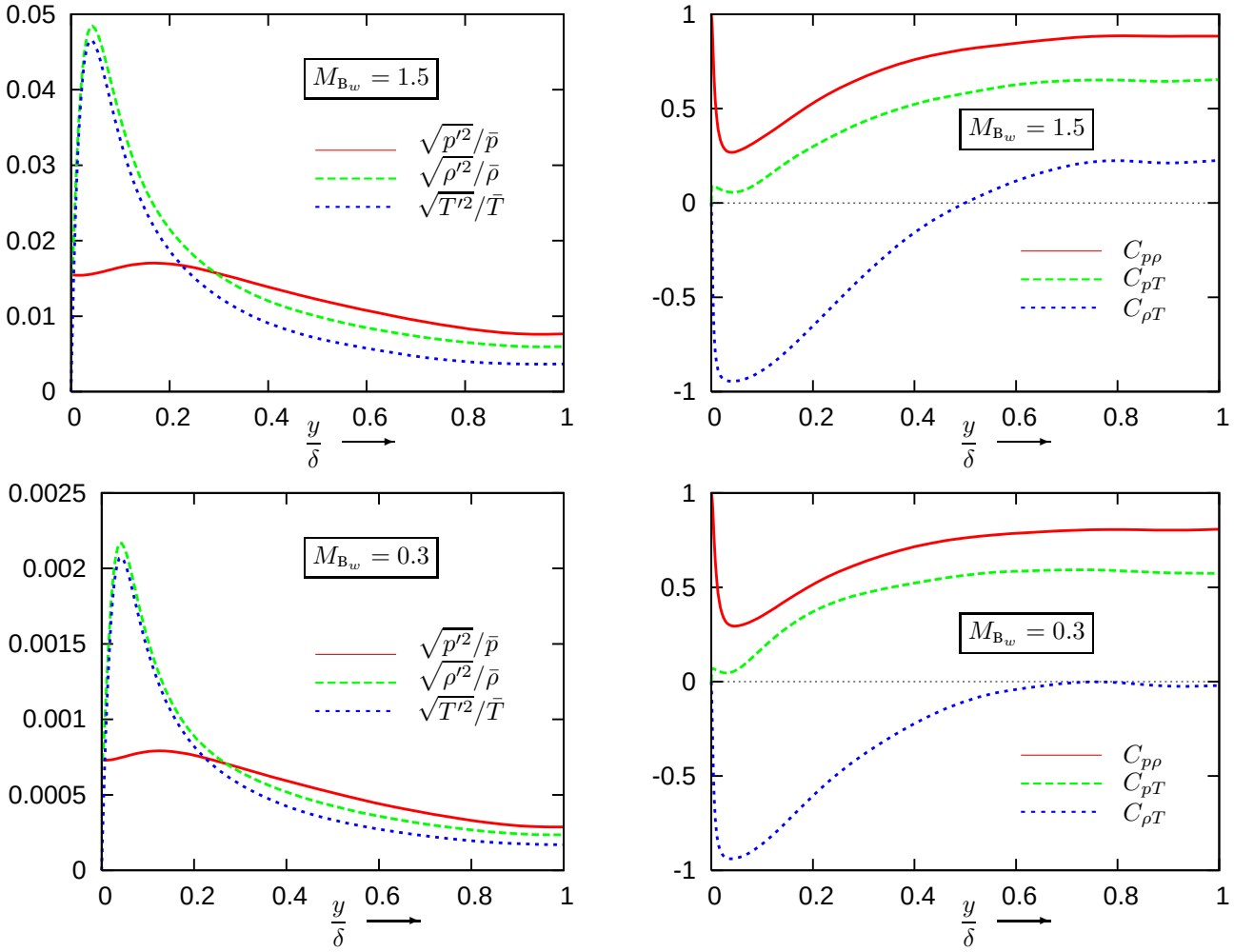

Figure 3. Relative levels of $p_{\rm rms}$, $\rho_{\rm rms}$, $T_{\rm rms}$, and correlation coefficients $C_{p\rho}$, $C_{\rho T}$, C_{pT} from the present low-subsonic Mach-number DNS computations ($Re_{\tau_w} = 230$; $M_{B_w} = 0.3,\ 1.5$).

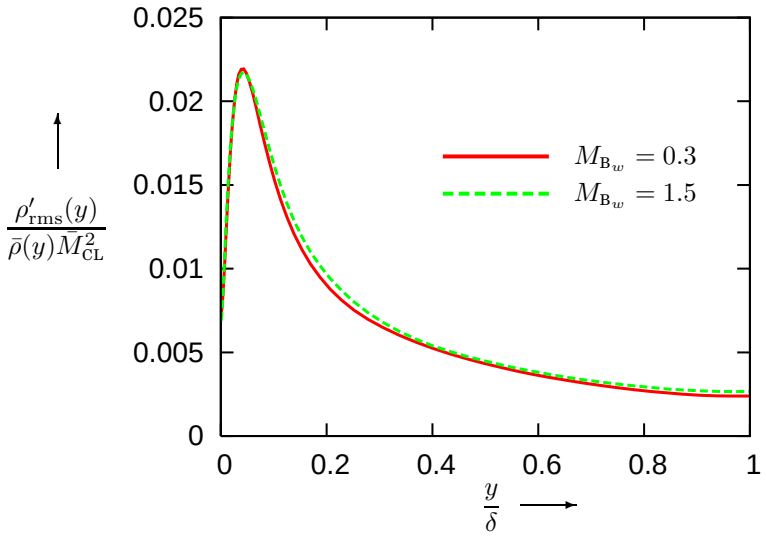

Figure 4. Density-variance scaling with average-centerline-Mach-number $\bar{M}_{\rm CL}$, $\rho'_{\rm rms}(y)/\bar{\rho}(y)/\bar{M}^2_{\rm CL}$, from the present low-subsonic ($Re_{\tau_w} = 230$; $M_{B_w} = 0.3$) and supersonic ($Re_{\tau_w} = 230$; $M_{B_w} = 1.5$) Mach-number DNS computations.

are directly obtained by the equation of state (Eq. 5)

$$p' = R_g\left(\rho' T' + \rho' \bar{T} + \bar{\rho} T' - \overline{\rho' T'}\right) \tag{17}$$

$$\overline{p'^2} = R_g\left(\overline{p'\rho' T'} + \overline{p'\rho'}\bar{T} + \overline{p'T'}\bar{\rho}\right) \tag{18}$$

$$\overline{p'\rho'} = R_g\left(\overline{\rho'^2 T'} + \overline{\rho'^2}\bar{T} + \overline{\rho' T'}\bar{\rho}\right) \tag{19}$$

$$\overline{p'T'} = R_g\left(\overline{\rho' T'^2} + \overline{\rho' T'}\bar{T} + \overline{T'^2}\bar{\rho}\right) \tag{20}$$

$$\overline{p'T'} = R_g\left(\overline{\rho' T'^2} + \overline{\rho' T'}\bar{T} + \overline{T'^2}\bar{\rho}\right) \tag{21}$$

Density-fluctuations $\rho'_{\rm rms}(y)/\bar{\rho}(y)$ scale with $\bar{M}_{\rm CL}^{-2}$ (Fig. 4), but the relative importance of $\rho'_{\rm rms}(y)/\bar{\rho}(y)$ and of $p'_{\rm rms}(y)/\bar{p}(y)$ is independent of $\bar{M}_{\rm CL}$.

B. Density-Variance-Transport Budgets and Modelling

The density-variance equation, for the plane channel flow case (taking into account that $\tilde{v} = 0$ from the averaged continuity equation, and that $\breve{\Theta} = 0$) reads

$$\underbrace{\frac{d}{dy}(\overline{\rho'^2 v''})}_{d_{(\rho')}} \quad \underbrace{-\overline{\rho' v'}\frac{d\bar{\rho}}{dy}}_{P_{(\rho')} = P_{(\rho';\nabla\bar{\rho})}} \quad \underbrace{-\left[-\overline{\rho'^2 \frac{\partial u''_\ell}{\partial x_\ell}} + 2\overline{\rho\rho' \frac{\partial u''_\ell}{\partial x_\ell}}\right]}_{\varepsilon_{(\rho')} := \varepsilon_{(\rho';1)} + \varepsilon_{(\rho';2)}} = 0 \tag{22}$$

In this flow, in the absence of meanflow dilatation, density fluctuations are produced by the interaction of the fluctuating massflux $\overline{\rho'^2 v''}$ with the mean-density-gradients $d_y\bar{\rho}$. This production $P_{(\rho')} = P_{(\rho';\nabla\bar{\rho})}$) is counterbalanced by the combined acion of diffusion ($d_{(\rho')}$) and of destruction $\varepsilon_{(\rho')}$, as shown in the budgets obtained from the DNS computations (Fig. 5). Expectedly, turbulent diffusion from the transport of ρ'^2 by the fluctuating velocity vector u''_i gives a negative contribution (loss) to the $\overline{\rho'^2}$-balance in the region of high production (Fig. 5). The maximum of $P_{(\rho')}$ is located approximately at $y^+ = 10$, whereas the maximum of destruction is located at $y^+ = 7$, at least for the low-Reynolds-numbers studied in the present work (Fig. 5).

Compressibility tends to slightly increase the y^+-location of the maxima, as seen from the $M_{\mathrm{B}_w} = 1.5$ results (Fig. 5). It is nonetheless remarkable that there is almost no influence of the Mach-number on the importance of the various terms in the budgets of the $\overline{\rho'^2}$-transport (Fig. 5).

The isothermal-wall boundary-condition (Eq. 16), for the perfect-gas equation-of-state (Eq. 8), clearly indicates the coupling (through the isothermal-wall boundary-condition) between the pressure and the density fluctuations. Notice that $d_y\overline{\rho'^2} \neq 0$ (Figs. 3, 4), so that the equations for the $\overline{\rho'^2}$ and $\overline{p'^2}$ are coupled one-with-another, in the isothermal-wall case. The situation would be different, in the adiabatic-wall case, where 0-gradient boundary-conditions prevail. Nonetheless, the limiting form of the $\overline{\rho'^2}$-transport (Eq. 22), at the wall where the massflux $\overline{\rho' u'_i}$ vanishes because of the no-slip boundary-condition, reads

$$[d_{(\rho')}]_w - \overline{\rho'^2_w}\breve{\Theta}_w - [\varepsilon_{(\rho')}]_w = 0 \tag{23}$$

and this form of the equation may be used for modelling purposes (for the fully-developed plane-channel flow $\breve{\Theta} = 0$ so that (Eq. 23) simplifies to $[\varepsilon_{(\rho')}]_w = [d_{(\rho')}]_w = [d_y(\overline{\rho'^2 v''})]_w$.

Yoshizawa[23] models $\overline{\rho'^2}$-transport without explicitly accounting for production by meanflow-density-gradients. It is not clear how the modelled equation of Yoshizawa[23] accounts for the associated production, which is important in the near-wall region (Fig. 5), and, for the present fully-developed plane-channel flow is the only production mechanism.

Taulbee and VanOsdol[18] have modelled the density-variance-equation, with an associated model for the turbulent massflux $\overline{u''_i} = -\overline{\rho' u'_i}(\bar{\rho})^{-1}$. A boundary-layer implementation of the model was used, in conjunction with a $\mathrm{k}-\varepsilon$ model for the meanflow equations, to compare with the experimental measurements of Kistler.[?] The closures used by Taulbee and VanOsdol[18] were

$$\overline{\rho'^2 u''_i} \models -\mu_{\mathrm{T}}\frac{\partial}{\partial y}\left(\frac{\overline{\rho'^2}}{\bar{\rho}}\right) \quad ; \quad \mu_{\mathrm{T}} = C_\mu\frac{\mathrm{k}^2}{\varepsilon^*} \quad ; \quad C_\mu = 0.09 f_\mu = 0.09\left\{1 - e^{-0.0115 y^+}\right\} \tag{24}$$

$$\varepsilon_{(\rho')} \models C_{(\varepsilon_{\rho'})}(y^+)\frac{\varepsilon^*}{\mathrm{k}}\overline{\rho'^2} \quad ; \quad C_{(\varepsilon_{\rho'})} = \frac{5.3}{f_\mu(y^+)} \quad ; \quad \varepsilon^* = \varepsilon - 2\nu\frac{\mathrm{k}}{y^2} \tag{25}$$

where $\mu_T \bar{\rho} \nu_T$ was taken from the k $-$ ε model of Chien,[34] and $C_{\varepsilon_{(\rho')}}(y^+)$ contains an anti-damping function of y^+, such that $\lim_{y^+ \longrightarrow 0} C_{\varepsilon_{(\rho')}} = \infty$. Although this model[18] was developed by a trial-and-error procedure (in the absence, at that time, of reliable near-wall data for $\overline{\rho'^2}$ and for the various terms appearing in the density-variance equation), this choice was made[18] in an attempt to reproduce the near-wall peak of $\varepsilon_{(\rho')}$ (Fig. 5).

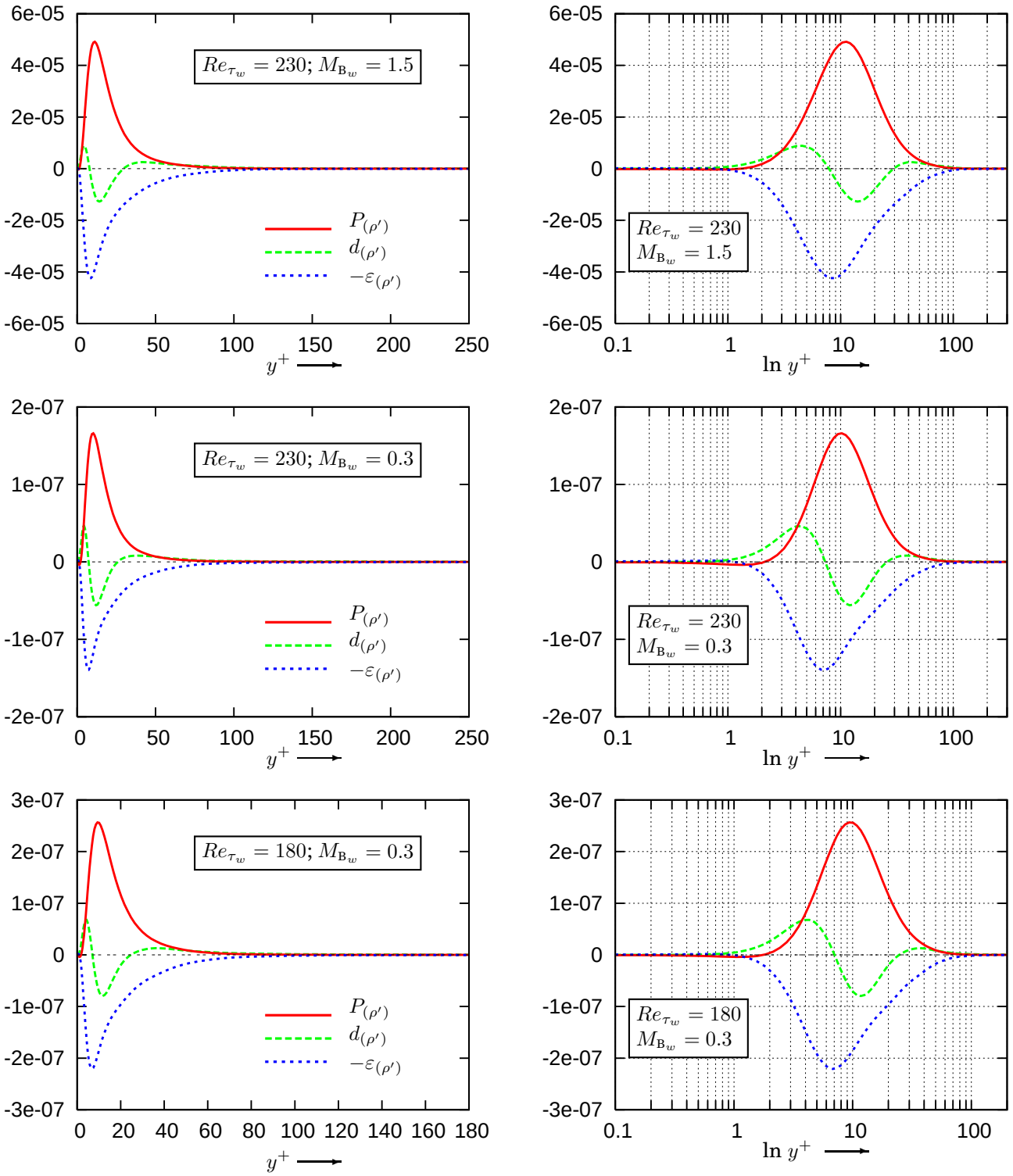

Figure 5. Budgets of various terms appearing in the $\overline{\rho'^2}$ transport equation using results from the present DNS computations.

A priori assessment of the model for $d_{(\rho')}$ (Eq. 24) against the present DNS data (Fig. 6) shows that the

model captures the form of $d_{(\rho')}$ in the near-wall region, but largely overestimates the magnitude of $d_{(\rho')}$. A recalibration of the model by a coefficient and/or the use of an alternative model proportional to $d_y\overline{\rho'^2}$ would solve this problem.

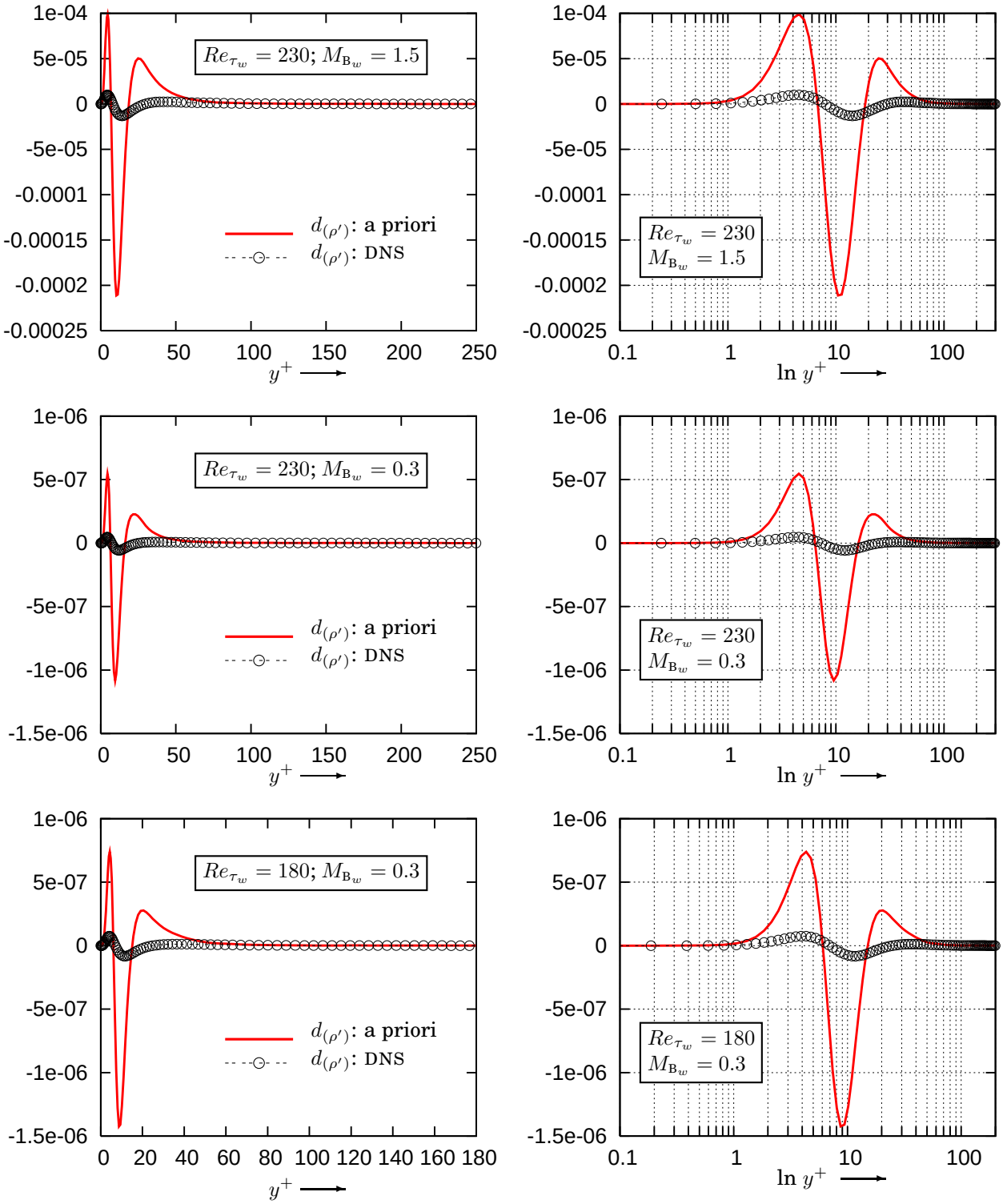

Figure 6. *A priori* comparison of the model of Taulbee and VanOsdol[18] for $d_{(\rho')}$.

A priori assessment of the model for $\varepsilon_{(\rho')}$ (Eq. 25) against the present DNS data (Fig. 7) shows that the model is quite unsatisfactory (curves $\div f_\mu$; Fig. 7). This is due to the fact that the original model, in the absence of DNS data at that time,[18] optimized the coefficient $C_{(\varepsilon_{\rho'})}$ to counterbalance the overestimated near-

wall anti-diffusion $d_{(\rho')}$ (Fig. 6). Using the same model (Eq. 25) without anti-damping ($C_{(\varepsilon_{\rho'})} = 5.3$) slightly improves the agreement (curves $f_\mu = 1$; Fig. 7), while the model with damping ($C_{(\varepsilon_{\rho'})} = 5.3 f_\mu(y^+)$) gives the correct near-wall form of $\varepsilon_{(\rho')}$, but requires reoptimization to give the correct level (curves $\times f_\mu$; Fig. 7).

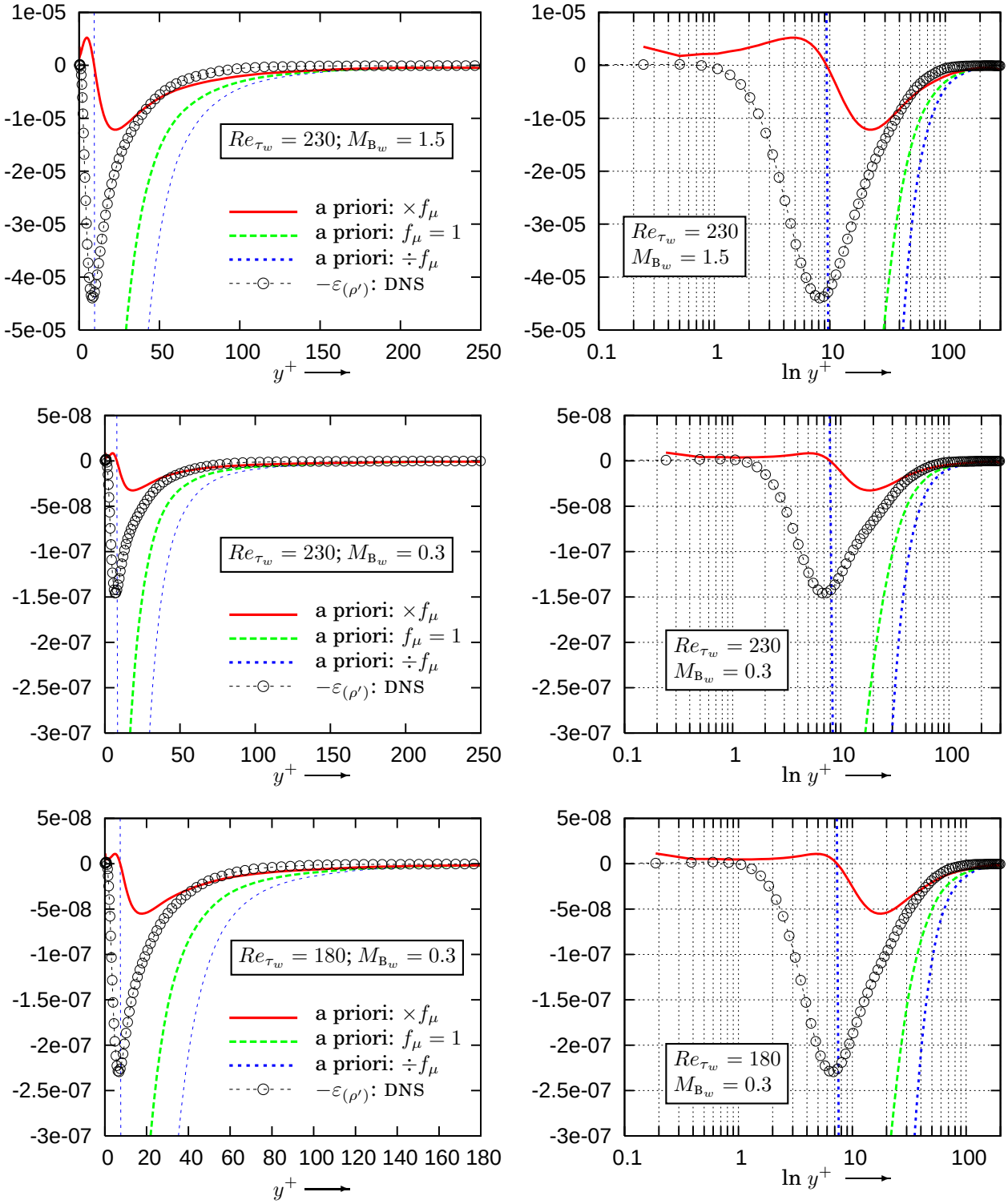

Figure 7. *A priori* comparison of the model of Taulbee and VanOsdol[18] for $\varepsilon_{(\rho')}$.

C. Budgets of Pressure-Variance Transport

Budgets of $\overline{p'^2}$-transport (Eq. 12) indicate (Fig. 8 that the pressure-dilatation correlation and especially the term $-3\gamma\phi_p$ is important in the near-wall region, both at supersonic and low-subsonic Mach-numbers. These results, are still being investigated, to ensure full convergence of the computations, because the $\overline{p'^2}$-budgets, and in general statistics of the p'-related terms, are the slowest to converge, especially for the low-Mach-number cases.

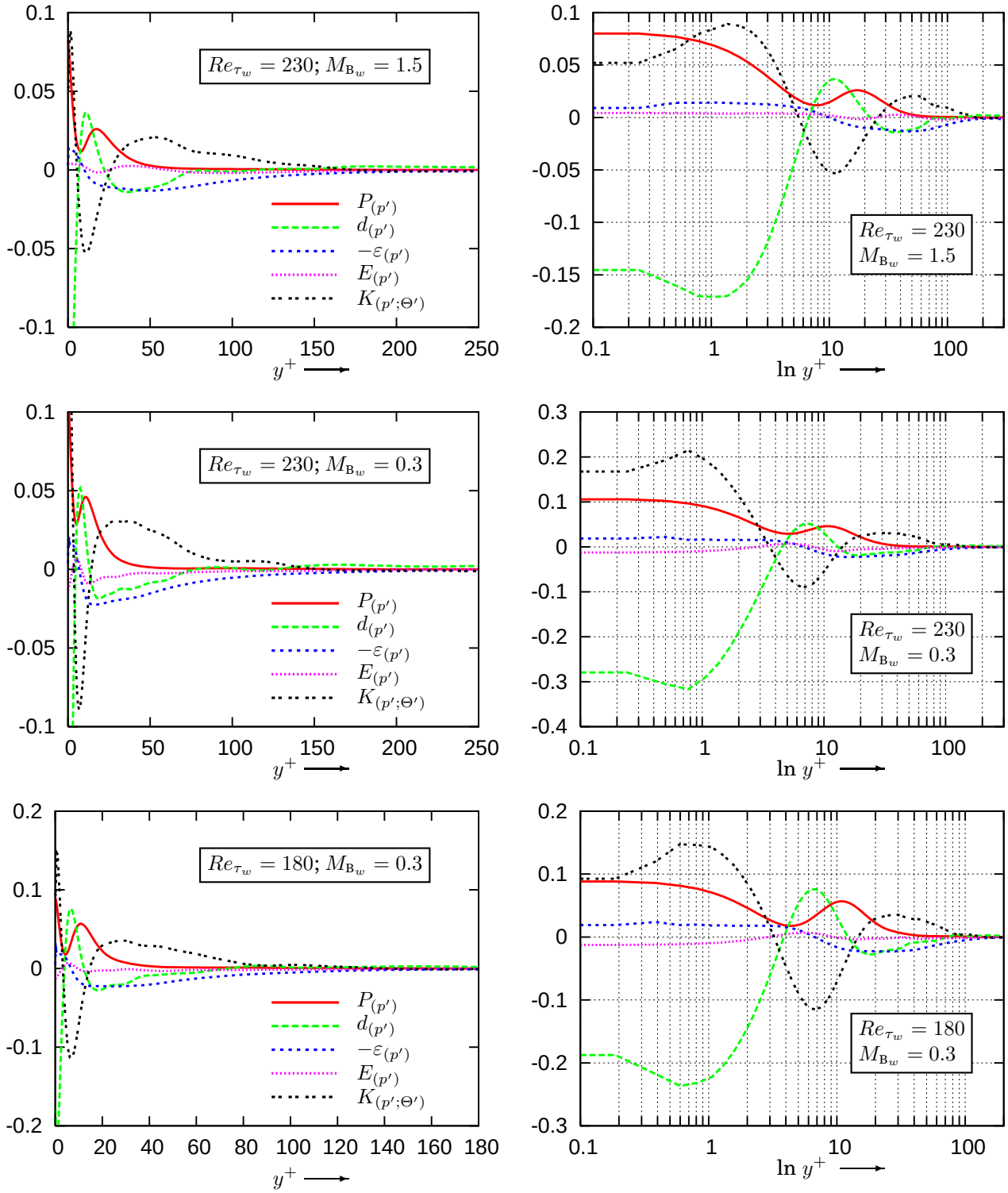

Figure 8. Budgets of various terms appearing in the $\overline{p'^2}$-transport (Eq. 12) using results from the present DNS computations.

D. Budgets of Pressure-Variance Transport

Budgets of $\widetilde{T''^2}$-transport (Eq. 15) indicate (Fig. 9) that the compressibility-related terms are important only in the supersonic case. The budgets obtained for the $\widetilde{T''^2}$-transport (Fig. 9) are in good agreement with the results of Tamano and Morinishi.[24]

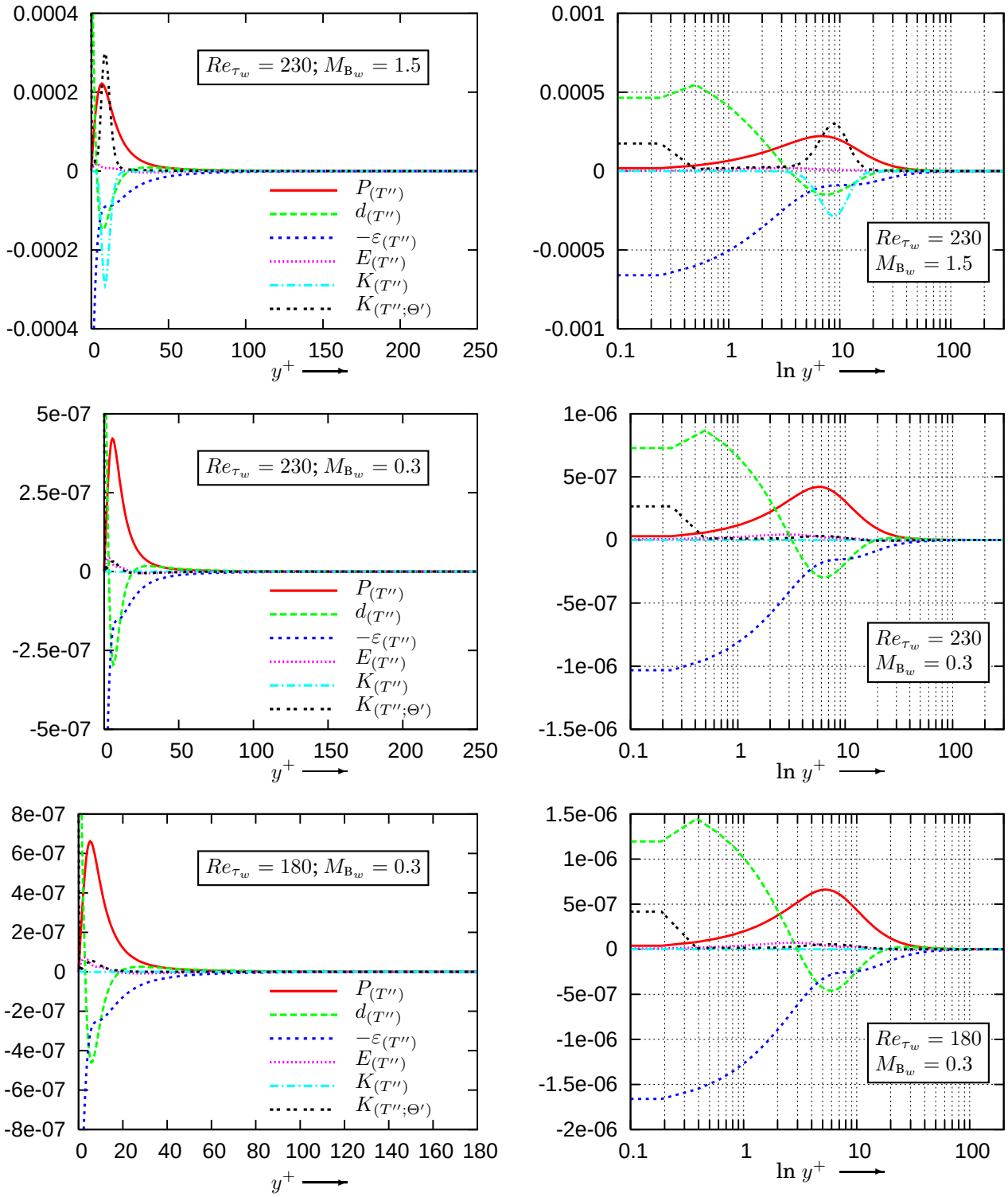

Figure 9. Budgets of various terms appearing in the $\widetilde{T''^2}$-transport (Eq. 15) using results from the present Mach-number DNS computations.

V. Conclusions

The present work studies the behaviour of density, pressure and temperature fluctuations in fully-developed compressible turbulent channel flow, over isothermal-walls based on low-Reynolds-number DNS computations, both at low-subsonic ($\bar{M}_{\rm CL} = 0.34$) and supersonic ($\bar{M}_{\rm CL} = 1.5$) conditions.

Results indicate that the near-wall behaviour of $\rho'_{\rm rms}/\bar{\rho}$, $p'_{\rm rms}/\bar{p}$, and $T'_{\rm rms}/\bar{T}$ is largely independent of Mach-number, although the fluctuation levels scale with $\bar{M}_{\rm CL}^-2$. This apparent compressibility, even at the low-Mach-number limit may be related to the isothermal-wall boundary-condition $\gamma p'_w = \bar{a}_w^2 \rho'_w$, which strongly couples ρ' and p', in the near-wall region. Even at the limit $\bar{M}_{\rm CL} \longrightarrow 0$, the ration ρ'_w/p'_w remains unchanged, suggesting that the equations for $\overline{p'^2}$ and for $\overline{\rho'^2}$ must be studied together.

Budgets of the transport-equations for $\overline{\rho'^2}$, $\overline{p'^2}$, and $\widetilde{T''^2}$ are obtained from the DNS computations. Comparison of previously proposed models for $\overline{\rho'^2}$-transport with the present DNS results suggests ways for improving these models, especially in the near-wall region.

Future work will concentrate both in enlarging the DNS database (various values of $\bar{M}_{\rm CL}$ and of Re_{τ_w}, including adiabatic-wall computations), and in developing single-point closures for the variances-transport equations.

Acknowledgments

The present work was conducted within the EU-funded research project ProBand, coordinated by Dr. L. Enghardt (DLR). The computations presented were run at the Institut pour le Développement des Ressources en Informatique Scientifique (IDRIS), where computer ressources were made available by the Comité Scientifique. The authors are listed alphabetically.

References

[1]Chang, III, P. A., Piomelli, U., and Blake, W. K., "Relations between Wall-Pressure and Velocity-Field Sources," *Phys. Fluids*, Vol. 11, No. 11, Nov. 1999, pp. 3434–3448.

[2]Hu, Z. W., Morfey, C. L., and Sandham, N. D., "Aeroacoustics of Wall-Bounded Turbulent Flow," *AIAA J.*, Vol. 40, No. 3, March 2002, pp. 465–473.

[3]Hu, Z. W., Morfey, C. L., and Sandham, N. D., "Sound Radiation in Turbulent Channel Flows," *J. Fluid Mech.*, Vol. 475, 2003, pp. 269–302.

[4]Hu, Z. W., Morfey, C. L., and Sandham, N. D., "Wall Pressure and Shear Stress Spectra from Direct Simulations of Channel Flow," *AIAA J.*, Vol. 44, No. 7, July 2006, pp. 1541–1549.

[5]Chou, P. Y., "On Velocity Correlations and the Solutions of the Equations of Turbulent Fluctuations," *Quart. Appl. Math.*, Vol. 3, 1945, pp. 38–54.

[6]Kim, J., "On the Structure of Pressure Fluctuations in Simulated Turbulent Channel-Flow," *J. Fluid Mech.*, Vol. 205, 1989, pp. 421–451.

[7]Bender, C. M. and Orszag, S. A., *Advanced Mathematical Methods for Scientists and Engineers*, Springer, New York [NY, USA], 1978, pp. 16–19.

[8]Foysi, H., Sarkar, S., and Friedrich, R., "Compressibility Effects and Turbulence Scalings in Supersonic Channel Flow," *J. Fluid Mech.*, Vol. 509, 2004, pp. 207–216.

[9]Gerolymos, G. A., Sénéchal, D., and Vallet, I., "Pressure Fluctuations in Quasi-Incompressible and Compressible Turbulent Plane Channel Flow," AIAA Paper 2007–3863, 37. AIAA Fluid Dynamics Conference, 25–28 jun 2007, Miami [FL, USA], June 2007.

[10]Hanjalić, K., "Advanced Turbulence Closure Models: A View of Current Status and Future Prospects," *Int. J. Heat Fluid Flow*, Vol. 15, 1994, pp. 178–203.

[11]Gerolymos, G. A. and Vallet, I., "Advances in the Numerical Computation of Complex Flows using Reynolds-Stress Models," AIAA Paper 2007–3963, 18. AIAA Computational Fluid Dynamics Conference, 25–28 jun 2007, Miami [FL, USA], June 2007.

[12]Senthooran, S., Lee, D. D., and Parameswaran, S., "A Computational Model to Calculate the Flow-Induced Pressure Fluctuations on Buildings," *J. Wind Eng. Ind. Aerodyn.*, Vol. 92, 2004, pp. 1131–1145.

[13]Chen, Y. S., "A Root-Mean-Square Pressure Fluctuations Model for Internal Flow Applications," Contr. Rep. NASA–CR–1985-3928, NASA, Marshall Space Flight Center,[USA], Sept. 1985.

[14]Hamba, F., "Effects of Pressure Fluctuations on Turbulence Growth in Compressible Homogeneous Shear Flow," *Phys. Fluids*, Vol. 11, No. 6, June 1999, pp. 1623–1635.

[15]Gerolymos, G. A., Sénéchal, D., and Vallet, I., "DNS of Compressible Channel Flow using Low-Diffusion High-Order Upwind Schemes," AIAA Paper 2007–4196, 18. AIAA Computational Fluid Dynamics Conference, 25–28 jun 2007, Miami [FL, USA], June 2007.

[16]Pantano, C. and Sarkar, S., "A Study of Compressibility Effects in the High-Speed Turbulent Shear Layer using Direct Simulation," *J. Fluid Mech.*, Vol. 451, 2002, pp. 329–371.

[17]Strahle, W. C., "Pressure-Strain and Pressure-Scalar Gradient Correlations in Variable-Density Turbulent Flows," *AIAA J.*, Vol. 26, 1988, pp. 969–973.

[18]Taulbee, D. and VanOsdol, J., "Modeling Turbulent Compressible Flows: The Mass Fluctuating Velocity and Squared Density," AIAA Paper 91–0524, 1991.

[19]Lee, J., Taulbee, D. B., and Holden, M. S., "Study of Turbulence on Supersonic Compression Surfaces using Reynolds Stress Model," *AIAA J.*, Vol. 30, No. 7, July 1992, pp. 1738–1746.

[20]Adumitroaie, V., Ristorcelli, J. R., and Taulbee, D. B., "Progress in Favre-Reynolds Stress Closures for Compressible Flows," *Phys. Fluids*, Vol. 11, No. 9, Sept. 1999, pp. 2696–2719.

[21]Smits, A. J. and Dussauge, J. P., *Turbulent Shear Layers in Supersonic Flow*, Springer, New York [NY, USA], 2006.

[22]Gerolymos, G. A., Sénéchal, D., and Vallet, I., "RSM–VLES Multiblock Implicit Solver using High-Order Upwind Schemes," AIAA

Paper 2006–3909, 36. AIAA Fluid Dynamics Conference, 5–8 jun 2006, San Fransisco [CA, USA], June 2006, (submitted to *AIAA J.*).

[23]Yoshizawa, A., "3-Equation Modeling of Inhomogeneous Compressible Turbulence based on a 2-Scale Direct-Interaction Approximation," *Phys. Fluids A*, Vol. 2, No. 5, May 1990, pp. 838–850.

[24]Tamano, S. and Morinishi, Y., "Effect of Different Thermal Wall Boundary-Conditions on Compressible Turbulent Channel Flow at $M = 1.5$," *J. Fluid Mech.*, Vol. 548, 2006, pp. 361–373.

[25]Kim, J., Moin, P., and Moser, R., "Turbulence Statistics in Fully Developed Channel Flow at Low-Reynolds-Number," *J. Fluid Mech.*, Vol. 177, 1987, pp. 133–166.

[26]Moser, R. D., Kim, J., and Mansour, N. N., "Direct Numerical Simulation of Turbulent Channel Flow up to $Re_\tau = 590$," *Phys. Fluids*, Vol. 11, No. 4, April 1999, pp. 943–945.

[27]Coleman, G. N., Kim, J., and Moser, R. D., "A Numerical Study of Turbulent Supersonic Isothermal-Wall Channel Flow," *J. Fluid Mech.*, Vol. 305, 1995, pp. 159–183.

[28]Chassaing, J. C., Gerolymos, G. A., and Vallet, I., "Reynolds-Stress Model Dual-Time-Stepping Computation of Unsteady 3-D Flows," *AIAA J.*, Vol. 41, No. 10, Oct. 2003, pp. 1882–1894.

[29]Gerolymos, G. A., "Implicit Multiple-Grid Solution of the Compressible Navier-Stokes Equations using $\mathrm{k} - \varepsilon$ Turbulence Closure," *AIAA J.*, Vol. 28, No. 10, Oct. 1990, pp. 1707–1717.

[30]Lechner, R., Sesterhenn, J., and Freidrich, R., "Turbulent Supersonic Channel Flow," *J. Turb.*, Vol. 2, 2001, pp. 001.1–001.25.

[31]Hu, Z. W. and Sandham, N. D., "DNS Databases for Turbulent Couette and Poiseuille Flow," Tech. Rep. AFM–01–04, AFM Research Group, School of Engineering Sciences, University of Southampton, aug 2001.

[32]Huang, P. G., Coleman, G. N., and Bradshaw, P., "Compressible Turbulent Channel Flows: DNS Results and Modelling," *J. Fluid Mech.*, Vol. 305, 1995, pp. 185–218.

[33]Pope, S. B., *Turbulent Flows*, Cambridge University Press, Cambridge [GBR], 2000.

[34]Chien, K. Y., "Predictions of Channel and Boundary-Layer Flows with a Low-Reynolds Number Turbulence Model," *AIAA J.*, Vol. 20, No. 1, Jan. 1982, pp. 33–38.